

Magnetic fields in the Galactic halo bubbles and deflections of UHECRs

Vasundhara Shaw,^{a,b} Arjen van Vliet^{c,*} and Andrew M. Taylor^a

^aDeutsches Elektronen-Synchrotron, Platanenallee 6, Zeuthen, Germany

^bUniversity of Potsdam, Institute of Physics and Astronomy, 14476 Potsdam, Germany

^cDepartment of Physics, Khalifa University, P.O. Box 127788, Abu Dhabi, United Arab Emirates

E-mail: vasundhara.shaw@desy.de, arjen.vliet@ku.ac.ae,
andrew.taylor@desy.de

In this contribution, based on Ref. [1], we motivate a magnetic-field model in the Galactic-halo-bubbles region. Observations from Fermi-LAT [2–4] and eROSITA [5] show evidence of extended bubble-like structures in the Galactic-halo region, while WMAP [6], Planck [7], and S-PASS [8] also observed emission from extended Galactic structures at high Galactic latitudes. These non-thermal and thermal observations collectively motivate our investigation into the magnetic fields present in these Galactic halo bubbles. To constrain the parameters of our model, we combine it with an expression for the non-thermal electron distribution and generate sky maps of polarised synchrotron emission. These sky maps are then tested against Planck data at 30 GHz, showing the need for extended magnetic-field bubbles in the 2-10 μG range. Furthermore, we investigate the effect of these magnetic fields in the Galactic halo bubbles on the arrival directions of ultra-high-energy cosmic rays (UHECRs). We conclude that present uncertainties in the field strengths can have significant consequences on the arrival directions of the cosmic rays and thereby on the source localisation.

38th International Cosmic Ray Conference (ICRC2023)
26 July - 3 August, 2023
Nagoya, Japan



*Speaker

1. Introduction

Extended radio emission at high latitudes has been detected by the WMAP [6] and Planck [7] observatories and were coined the WMAP and Planck haze. S-PASS data confirmed the existence of extended Galactic radio emission, which was linked to giant magnetised outflows from the centre of our Galaxy [8]. Emission from giant outflows from the centre of the Milky Way was previously seen in gamma rays by Fermi LAT [2–4] and called the Fermi bubbles. Recently, eROSITA detected such large-scale bubbles extending from the Galactic centre in X-rays as well [5]. Here we call this extended structure detected in radio, gamma-ray and X-ray emission the Galactic halo bubbles.

Similar out-of-the-plane emission has been observed from other galaxies besides the Milky Way as well. For example from NGC 253, where extended structures have been observed in both radio and X-ray wavelengths [9, 10]. In addition, the radio survey CHANG-ES found extended (~ 10 kpc) halos in their survey of 35 external edge-on galaxies [11]. While Ref. [12] showed that halos with even larger sizes (hundreds of kpcs) are present around nearby spiral galaxies.

In Ref. [1], we provide a model for the magnetic fields in the Galactic halo bubbles. Magnetic fields in our Galaxy play a vital role in many astrophysical processes, including the propagation of cosmic rays through the Galaxy. One way to probe the magnetic fields in the Galactic halo bubbles is with synchrotron radiation, which is emitted by non-thermal cosmic-ray electrons due to their interactions with the local magnetic fields. The synchrotron radiation detected at Earth probes the magnetic-field component perpendicular to the line of sight from Earth to the source of the radiation.

Currently, our understanding of the magnetic fields in the Galactic halo is limited, compared to our knowledge of the magnetic fields in the Galactic disc. This is due to the lack of sources such as pulsars, starlight polarisation and dust emission in the halo that can be used to probe magnetic fields (see e.g. Ref. [13] for a review). However, indications for a toroidal magnetic field oriented in opposite directions above and below the Galactic plane have been found (see e.g. Refs. [14–16]). The large-scale magnetic fields outside of the Galactic plane are, therefore, often modelled as a toroidal component, possibly in combination with an X-shaped component, as for example in the widely-used model of Refs. [17, 18] (the JF12 model). This model, however, disregarded the region of the sky corresponding to the Galactic halo bubbles and focused on a large-scale halo field not associated with the bubbles near the Galactic centre. Here, we do the opposite and focus only on the Galactic-halo-bubbles region.

2. Magnetic-field model for the Galactic halo bubbles

In Ref. [1], we developed a magnetic-field model for the Galactic halo bubbles. This magnetic-field model consists of a large-scale axisymmetric structured toroidal field and small-scale turbulent fields. The structured field is described by the free parameters B_{str} , R_{mag} and Z_{mag} , with the total strength at a radial distance r from the Galactic centre in the xy plane and height z given by:

$$B_{\text{tor}}(r, z) = B_{\text{str}} e^{-|z|/Z_{\text{mag}}} e^{-z_{\text{min}}/|z|} e^{-r/R_{\text{mag}}}, \quad (1)$$

with the Galactic centre at $(0, 0, 0)$ and the Galactic disk in the xy plane. The Galactic plane is disregarded due to a fixed cut at $z_{\text{min}} = 100$ pc.

Table 1: Best-fit parameters for the model of the magnetic fields in the Galactic halo bubbles with 1σ uncertainties (with the lower limit of B_{str} reaching the scan boundary), adjusted from Ref. [1].

Parameter	Best-fit value	Description
B_{str}	$4_{-4}^{+7} \mu\text{G}$	Structured field strength
B_{tur}	$7_{-4}^{+10} \mu\text{G}$	Turbulent field strength
R_{mag}	5_{-0}^{+1}kpc	Radial cut off
Z_{mag}	6_{-0}^{+1}kpc	Azimuthal cut off
$\log_{10}(C_{\text{norm}}[\text{cm}^{-3}])$	$-11.7_{-0.9}^{+0.6}$	Electron density at 10 GeV

The turbulent component of the magnetic-field model is given by a Kolmogorov power-law spectrum with a coherence length of $L_{\text{coh}} = 150 \text{ pc}$. The RMS field strength B_{tur} of this component is treated as a free parameter. These turbulent fields extend out to 14 kpc from the Galactic centre so that they cover the entire Galactic bubble region as indicated by the eROSITA measurements [5]. One last free parameter in the model is the normalisation of the non-thermal electron density C_{norm} . See Ref. [1] for more details on the magnetic-field model and the electron-density distribution.

In Ref. [1], we calculated the polarised synchrotron emission for this setup as expected to arrive at Earth. We compared this to the publicly-available polarised radio data at 30 GHz from Planck. We scanned over the free parameters B_{str} , R_{mag} , Z_{mag} , B_{tur} and C_{norm} to obtain a best-fit result and allowed parameter ranges. The scan ranges of the different parameters were: from 2 kpc to 19 kpc in steps of 1 kpc for R_{mag} and Z_{mag} , from $2 \mu\text{G}$ to $18 \mu\text{G}$ logarithmically in 30 bins per decade for B_{str} and B_{tur} , and from 10^{-14} cm^{-3} to 10^{-11} cm^{-3} logarithmically with 10 bins per decade for C_{norm} . The results are summarised in Table 1.

The turbulent component of the magnetic-field model is not strongly constrained. The 1σ range for B_{tur} covers almost the entire scan range. However, the turbulent component is an essential component of the model. To illustrate the effect of the turbulent component, we show three different scenarios of polarised synchrotron emission in Fig. 1. These skymaps are smoothed using a Gaussian kernel with a size scale of 15° as we are only interested in the large-scale features, not the small-scale variations. The top figures only have turbulent magnetic fields with $B_{\text{tur}} = 10 \mu\text{G}$, while the bottom figure only has structured magnetic fields with $B_{\text{str}} = 10 \mu\text{G}$ and with $R_{\text{mag}} = Z_{\text{mag}} = 6 \text{ kpc}$. The figures with only turbulent fields clearly have a different morphology than the case with only structured fields and it is clear that the turbulent fields can add a significant amount of polarised emission to the overall sky. Comparing the skymaps of Fig. 1 with Fig. 3 of Ref. [1] shows that both structured and turbulent fields are necessary to get the morphology as close as possible to the Planck data.

The difference between the top-left and top-right figures is the cutoff distance of the turbulent fields. The top-left skymap has an exponential spatial cutoff in the same way as the structured fields (Eq. 1) with $R_{\text{mag}} = Z_{\text{mag}} = 6 \text{ kpc}$. The top-right skymap has volume-filled turbulent magnetic fields up to 14 kpc from the Galactic centre (as in the original magnetic-field model). A larger cutoff distance clearly increases the total polarised intensity.

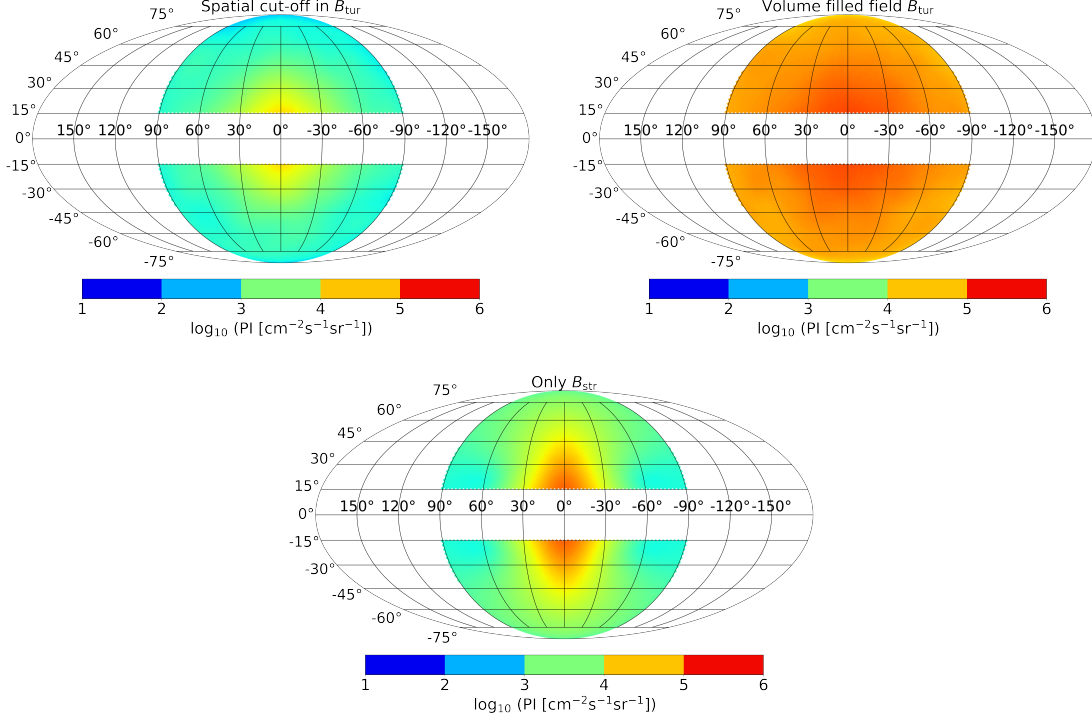


Figure 1: Polarised synchrotron skymaps for different Galactic-halo-bubble magnetic-field setups, smoothed on a size scale of 15° using a Gaussian kernel. **Top left:** Only turbulent fields with $B_{\text{tur}} = 10 \mu\text{G}$ and an exponential spatial cutoff the same as the structured-field model (Eq. 1) with $R_{\text{mag}} = Z_{\text{mag}} = 6 \text{ kpc}$. **Top right:** Only turbulent fields with $B_{\text{tur}} = 10 \mu\text{G}$, volume filled up to 14 kpc from the Galactic centre (as in the original magnetic-field model). **Bottom:** Only structured fields with $B_{\text{str}} = 10 \mu\text{G}$ and $R_{\text{mag}} = Z_{\text{mag}} = 6 \text{ kpc}$.

3. Deflections of UHECRs

To show the effects of the magnetic fields in the Galactic halo bubbles on UHECRs, we back-tracked UHECR trajectories from Earth through the magnetic-field model until the edge of the Galaxy using CRPropa 3 [19, 20]. In Ref. [1], we did this for two specific typical source candidates (Centaurus A and NGC 253). Here, we repeat this exercise for ten arbitrary source positions at a regular spacing ($l = -60^\circ, -30^\circ, 0^\circ, 30^\circ$ and 60° ; $b = -30^\circ$ and 30°). The results are shown in Fig. 2 for the best-fit magnetic-field model and both UHECR protons of 40 EeV and UHECR nitrogen nuclei of 40 EeV. The nitrogen nuclei show larger deviations from their original source positions due to the higher charge of nitrogen compared with protons. The UHECRs from the sources with non-zero longitude show an average shift towards $l = 0^\circ$ due to the structured fields. An average shift towards $b = 0^\circ$ is visible as well, especially for the sources at $l = 0^\circ$.

Furthermore, in Fig. 3 we compare UHECR deflections (nitrogen of 40 EeV) from Cen A and NGC 253 for the lower bound and upper bound of our Galactic-halo-bubbles magnetic-field model (see also Fig. 4 of Ref. [1]) with the JF12 model. For the JF12 model, we included all components of the field (toroidal halo field, X-field and turbulent fields, in contrast to Fig. E1 of Ref. [1] where we did not include the X-field) except for the disc field as we did not include a disc field in our magnetic-field model. Including the disc field will not affect the conclusions from this comparison.

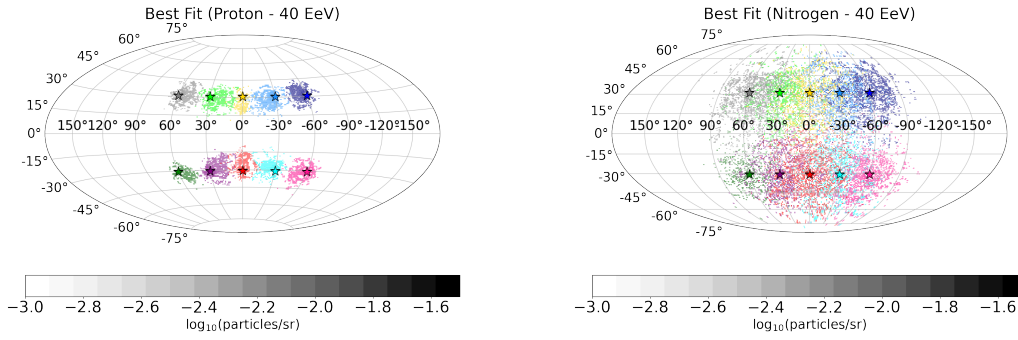


Figure 2: UHECR arrival directions for ten UHECR source positions on a regular grid, propagated through the best-fit magnetic-field model. **Left:** UHECR protons of 40 EeV. **Right:** UHECR nitrogen of 40 EeV.

From these sky maps, it is clear that the JF12 model causes larger shifts of the original source position for both sources than the Galactic-halo-bubbles model, while the Galactic-halo-bubbles model gives a larger spread around the source position. The larger shift is due to the stronger structured field in the JF12 case, while the larger spread is due to the stronger turbulent fields in the Galactic-halo-bubbles model.

4. Conclusions

In Ref. [1], we presented a model for the magnetic field in the Galactic halo bubbles, the giant magnetised outflows from the centre of the Milky Way. We determined the parameter ranges for which the polarised synchrotron emission best fits the polarised radio data at 30 GHz from Planck. This showed a rather well constrained radial extent and height of the bubbles, and the likely presence of both a structured and turbulent component of the magnetic field. In this work, we illustrate the effects of the turbulent component of this model of the Galactic-halo-bubbles magnetic fields on polarised synchrotron emission. Even though the RMS strength of the turbulent component is not well constrained, the turbulent component does provide an essential contribution to the intensity and morphology of the polarised synchrotron emission.

Furthermore, we investigate the effects that the Galactic-halo-bubble magnetic fields can have on the arrival directions of UHECRs. In Ref. [1], we showed this for two typical UHECR source candidates, Cen A and NGC 253. In this work, we repeat this exercise for ten arbitrary, regularly spaced, source positions. This shows the tendency for UHECRs to, on average, get deflected more towards $l = 0^\circ$ and $b = 0^\circ$.

We also compare the expected UHECR arrival directions for the Galactic-halo-bubble magnetic-fields model with the expected UHECR arrival directions for the widely-used JF12 Galactic-magnetic-field model for Cen A and NGC 253 as potential UHECR sources. On average, the shift of the source position is larger in the JF12 model, while the spread around the source position is larger in the Galactic-halo-bubble magnetic-fields model. If the overdensities around Cen A and NGC 253 in the distribution of UHECR arrival directions measured by the Pierre Auger Observatories [21, 22] are indeed produced by UHECRs from these two sources, then only a negligible shift of the original source position and a wide spread around the original source position are ob-

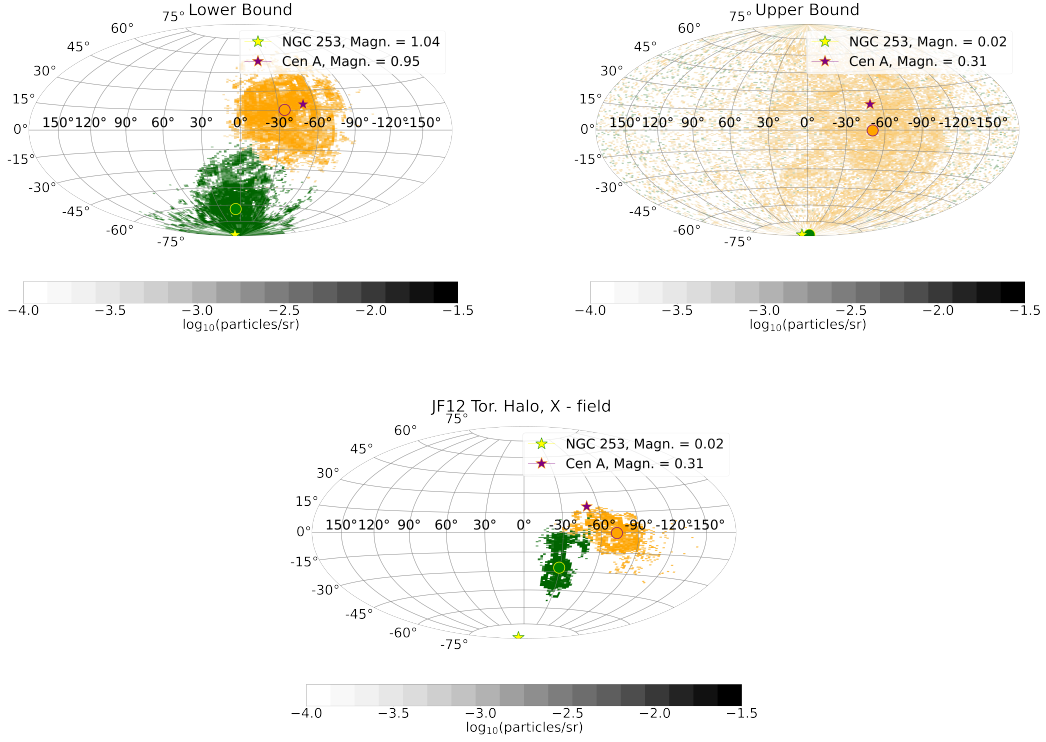


Figure 3: Simulated UHECR arrival directions, nitrogen of 40 EeV, for two potential UHECR sources: NGC 253 and Cen A. **Top left (right):** UHECRs propagated through the lower (upper) bound of the Galactic-halo-bubbles magnetic-field model, adopted from Ref. [1] with updated color-bar range for easier comparison. **Bottom:** UHECRs propagated through the JF12 Galactic-magnetic-field model, without the disc component of this model.

served. This is more consistent with a magnetic-field realisation similar to the Galactic-halo-bubble magnetic-fields model than with the JF12 model.

Acknowledgements

We would like to thank Mike Peel and Michael Unger for helpful discussions related to this work. This work benefited from discussions during the program "Towards a Comprehensive Model of the Galactic Magnetic Field" at Nordita in April 2023, which is partly supported by NordForsk and the Royal Astronomical Society. AvV acknowledges support from Khalifa University's FSU-2022-025 grant.

References

- [1] V. Shaw, A. van Vliet and A.M. Taylor, *Galactic halo bubble magnetic fields and UHECR deflections*, *Mon. Not. Roy. Astron. Soc.* **517** (2022) 2534 [2202.06780].

- [2] G. Dobler, D.P. Finkbeiner, I. Cholis, T.R. Slatyer and N. Weiner, *The Fermi haze: A gamma-ray counterpart to the microwave haze*, *Astrophys. J.* **717** (2010) 825 [0910.4583].
- [3] M. Su, T.R. Slatyer and D.P. Finkbeiner, *Giant gamma-ray bubbles from Fermi-LAT: AGN activity or bipolar Galactic wind?*, *Astrophys. J.* **724** (2010) 1044 [1005.5480].
- [4] M. Su and D.P. Finkbeiner, *Evidence for gamma-ray jets in the Milky Way*, *Astrophys. J.* **753** (2012) 61 [1205.5852].
- [5] P. Predehl et al., *Detection of large-scale X-ray bubbles in the Milky Way halo*, *Nature* **588** (2020) 227 [2012.05840].
- [6] D.P. Finkbeiner, *Microwave ISM emission observed by WMAP*, *Astrophys. J.* **614** (2004) 186 [astro-ph/0311547].
- [7] PLANCK collaboration, *Planck intermediate results. IX. Detection of the Galactic haze with Planck*, *Astron. Astrophys.* **554** (2013) A139 [1208.5483].
- [8] E. Carretti, R.M. Crocker, L. Staveley-Smith, M. Haverkorn, C. Purcell, B.M. Gaensler et al., *Giant magnetized outflows from the centre of the Milky Way*, *Nature* **493** (2013) 66 [1301.0512].
- [9] R. Beck, C.L. Carilli, M.A. Holdaway and U. Klein, *Multifrequency observations of the radio continuum emission from NGC 253. I. Magnetic fields and rotation measures in the bar and halo*, *Astron. Astrophys.* **292** (1994) 409.
- [10] W. Pietsch, A. Vogler, U. Klein and H. Zinnecker, *X-ray observations of the starburst galaxy NGC 253. II. Extended emission from hot gas in the nuclear area, disk, and halo*, *Astron. Astrophys.* **360** (2000) 24 [astro-ph/0005335].
- [11] M. Krause, J. Irwin, P. Schmidt, Y. Stein, A. Miskolczi, S. Carolina Mora-Partiarroyo et al., *CHANG-ES. XXII. Coherent magnetic fields in the halos of spiral galaxies*, *Astron. Astrophys.* **639** (2020) A112 [2004.14383].
- [12] J.N. Bregman, E. Hodges-Kluck, Z. Qu, C. Pratt, J.-T. Li and Y. Yun, *Hot extended galaxy halos around local l^* galaxies from sunyaev–zeldovich measurements*, *Astrophys. J.* **928** (2022) 14.
- [13] J. Han, *Observing interstellar and intergalactic magnetic fields*, *Annu. Rev. Astron. Astrophys.* **55** (2017) 111.
- [14] J.L. Han, R.N. Manchester, E.M. Berkhuijsen and R. Beck, *Antisymmetric rotation measures in our Galaxy: evidence for an A0 dynamo*, *Astron. Astrophys.* **322** (1997) 98.
- [15] L. Page, G. Hinshaw, E. Komatsu, M.R.olta, D.N. Spergel, C.L. Bennett et al., *Three-year Wilkinson Microwave Anisotropy Probe (WMAP) observations: Polarization analysis*, *Astrophys. J. Suppl.* **170** (2007) 335 [astro-ph/0603450].

- [16] X.H. Sun, W. Reich, A. Waelkens and T.A. Enßlin, *Radio observational constraints on Galactic 3D-emission models*, *Astron. Astrophys.* **477** (2008) 573 [0711.1572].
- [17] R. Jansson and G.R. Farrar, *A new model of the Galactic magnetic field*, *Astrophys. J.* **757** (2012) 14 [1204.3662].
- [18] R. Jansson and G.R. Farrar, *The Galactic magnetic field*, *Astrophys. J. Lett.* **761** (2012) L11 [1210.7820].
- [19] R. Alves Batista, A. Dundovic, M. Erdmann, K.-H. Kampert, D. Kuempel, G. Müller et al., *CRPropa 3 - a public astrophysical simulation framework for propagating extraterrestrial ultra-high energy particles*, *JCAP* **05** (2016) 038 [1603.07142].
- [20] R. Alves Batista et al., *CRPropa 3.2 - an advanced framework for high-energy particle propagation in extragalactic and galactic spaces*, *JCAP* **09** (2022) 035 [2208.00107].
- [21] PIERRE AUGER collaboration, *Searches for anisotropies in the arrival directions of the highest energy cosmic rays detected by the Pierre Auger Observatory*, *Astrophys. J.* **804** (2015) 15 [1411.6111].
- [22] PIERRE AUGER collaboration, *Arrival directions of cosmic rays above 32 EeV from phase one of the Pierre Auger Observatory*, *Astrophys. J.* **935** (2022) 170 [2206.13492].